



1 Satellite-based estimate of the variability of warm cloud 2 properties associated with aerosol and meteorological 3 conditions

4 Yuqin Liu^{1,2}, Jiahua Zhang^{2,3}, Putian Zhou⁵, Tao Lin^{1,6}, Juan Hong⁷, Lamei Shi^{2,3},
5 Fengmei Yao³, Huadong Guo², Gerrit de Leeuw^{4,5}

6 ¹Key Lab of Urban Environment and Health, Institute of Urban Environment, Chinese Academy of Sciences, Xiamen 361021, China

7 ²Institute of Remote Sensing and Digital Earth, Chinese Academy of Sciences, Beijing, China

8 ³University of Chinese Academy of Sciences, Beijing, China

9 ⁴Finish Meteorological Institute, Climate Change Unit, P.O. Box 503, 00101 Helsinki, Finland

10 ⁵Department of Physics, P.O. Box 64, 00014 University of Helsinki, Helsinki, Finland

11 ⁶Xiamen Key Lab of Urban Metabolism, Xiamen 361021, China

12 ⁷Institute for Environmental and Climate Research, Jinan University, Guangzhou, Guangdong 511443, China

13 *Correspondence to:* Jiahua Zhang (zhangjh@radi.ac.cn)

14
15 **Abstract.** Aerosol-cloud interaction is examined using four years of data from the MODIS/Terra (morning
16 orbit) and MODIS/Aqua (afternoon orbit) satellites. Aerosol optical depth (AOD) and cloud properties
17 retrieved from both sensors are used to explore in a statistical sense the morning-to-afternoon variation of
18 cloud properties in conditions with low and high AOD, over both land and ocean. The results show that the
19 morning-to-afternoon variation of cloud properties during the 3 hours between the Terra and Aqua
20 overpasses have similar patterns (increase or decrease) over land under both low and high AOD conditions.
21 The variation in $d(\text{Cloud}_X)$, defined as the mean change in cloud property Cloud_X between the morning
22 and afternoon overpasses in high AOD conditions minus that in low AOD conditions, is different over land
23 and ocean. This applies to cloud droplet effective radius (CDR), cloud fraction (CF) and cloud top pressure
24 (CTP), but not to cloud optical thickness (COT) and cloud liquid water path (CWP). The effects of initial
25 cloud fraction and meteorological conditions on the change in CF are also explored, showing that upward
26 motion of air parcels can enhance the cloud cover much more when AOD is high than when it is low. In
27 contrast, the increase of cloud cover with increasing relative humidity is much stronger in a relatively clean
28 atmosphere with low AOD than in a more polluted atmosphere. Meanwhile, stable atmospheric conditions
29 favour the development of a low cloud cover, especially when AOD is high. Overall, the analysis of the
30 diurnal variation of cloud properties provides a better understanding of aerosol-cloud interaction over land
31 and ocean.

32 **Key words:** MODIS, cloud development, aerosol-cloud interaction, urban clusters, ocean

33 1 Introduction

34 Clouds and cloud systems are crucial elements in the energy cycle of our planet (Hartmann et al., 1992;
35 Webb et al., 2006). Clouds affect the global energy budget by reflecting incoming solar radiation, and thus
36 cool the Earth surface, and by absorption and re-emitting outgoing terrestrial radiation which contributes to
37 warming of the surface. In addition to the radiative effects, clouds also influence the hydrological cycle of
38 the Earth through precipitation (Stephens et al., 2002). Due to interactions with aerosols, the climatic effects
39 of clouds are further complicated (Rosenfeld, 2000; Twomey, 2007). Aerosols can serve as cloud
40 condensation nuclei (CCN), depending on their hygroscopic properties, and when activated they can change
41 the cloud microphysical properties. The increase of CCN, while the liquid water path remains constant,



1 usually results in more numerous cloud droplets with smaller cloud droplet radius (CDR) due to the
2 competition for the same amount of water vapour. Thus, cloud albedo increases and the smaller cloud
3 droplet effective radius results in the suppression of precipitation, which in turn results in a longer cloud
4 lifetime, and maintaining a larger liquid water path (Albrecht, 1989; Feingold et al., 2001). Therefore, it is
5 important to understand the interaction between aerosols and clouds and the effect of different processes on
6 cloud development.

7 Numerous studies have shown that aerosol particles can affect cloud properties on regional and global scales
8 (Krüger and Graßl, 2002; Menon et al., 2008; Rosenfeld et al., 2014; Sporre et al., 2014; Saponaro et al.,
9 2017). Satellite measurements suggest that the cloud droplet effective radius (CDR) decreases with
10 increasing aerosol optical depth (AOD, which is used in this paper as a proxy for aerosol concentration),
11 which is consistent with Twomey's theory (Kaufman et al., 2005; Matheson et al., 2005; Meskhidze and
12 Nenes, 2010). However, other observational and model studies reported that CDR tends to increase with
13 aerosol loading in some study areas, especially over land (Feingold et al., 2001; Yuan et al., 2008; Grandey
14 and Stier, 2010; Liu et al., 2017). A different behaviour of cloud cover as a function of AOD for different
15 aerosol loadings (low or high) has been found by Kaufman and Koren (2006) and Koren et al. (2008).
16 However, the observed correlations between aerosol and cloud cannot be simply attributed to the effects of
17 aerosols on clouds alone since other factors such as variations in meteorological conditions could play a role
18 (Loeb and Schuster, 2008; Reutter et al., 2009; Koren et al., 2010; Su et al., 2010; Stathopoulos et al., 2017).
19 "Snapshot" studies, where the aerosol and cloud properties are retrieved at the same time, have the
20 advantage that they represent the total time-integrated effect of aerosols on cloud properties (Meskhidze et
21 al., 2009; Gryspeerd et al., 2014). However, the use of "snapshot" correlations is limited to a single
22 overpass time and limits the ability to distinguish aerosol-cloud interactions from meteorological
23 covariation or retrieval errors (Gryspeerd et al., 2014). Therefore, the history of meteorological forcing is
24 an important determinant of cloud state. Matsui et al. (2006) investigated the properties of low clouds
25 derived from semiglobal observations by the Tropical Rainfall Measurement Mission (TRMM) and
26 explored the correlations of these cloud properties with aerosols (as indicated by the aerosol index or AI)
27 and with lower-tropospheric stability (LTS) on a diurnal scale. They found that aerosols affect the CDR
28 stronger for low LTS than for high LTS. Mauger and Norris (2007) used MODIS/Terra data to examine the
29 evolution of marine boundary layer clouds over several days but they may have missed important effects
30 occurring on a sub-daily timescale. Meskhidze et al. (2009) investigated the evolution of cloud properties
31 between the MODIS/Terra and MODIS/Aqua overpasses as a function of MODIS/Terra AOD and found an
32 apparent increase in the breakup rate of stratocumulus clouds in high AOD environments. However, they
33 did not explain meteorological covariation that may generate spurious correlations.

34 Considering the complex aerosol composition and increasing aerosol trend during the last decades over
35 eastern China (Guo et al., 2011), a systematic assessment of the effect of aerosols on the properties of warm
36 clouds is desperately needed, over both land and ocean. In this paper, aerosol-cloud interaction is examined
37 using multi-year statistics of remotely sensed data from the two MODIS sensors aboard NASA's Terra
38 (daytime equator crossing time at 10:30 LT) and Aqua (daytime equator crossing time at 13:30 LT)
39 satellites. The retrieval of the AOD and cloud properties from both sensors allows us to explore the
40 morning-to-afternoon variation of cloud properties in conditions with either low or high AOD, over land and
41 over ocean, and for different climate regimes. This variety of conditions allows us to identify similarities



1 and differences in the effects of aerosols on clouds and thus better understand aerosol-cloud interaction. We
2 also explore the effect of meteorological history on the interaction between aerosols and clouds. In this
3 paper, we focus on low-level water clouds. The paper is organized as follows. The data and region of interest
4 are described in Section 2. The main methodology is introduced in section 3. The results and analysis are
5 presented in section 4. Overall conclusions and potential future improvements are discussed in section 5.

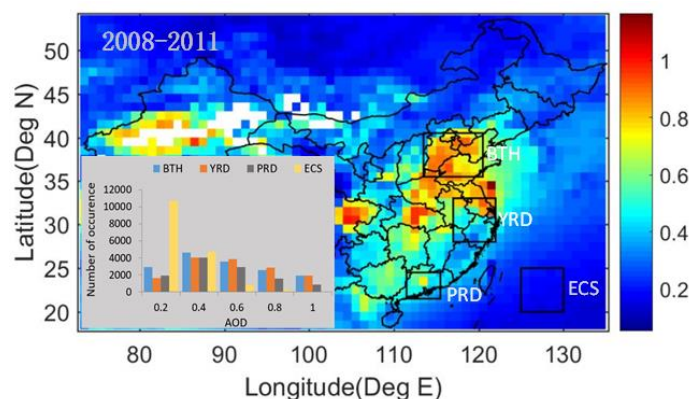
6 **2 Approach**

7 **2.1 Study area**

8 Aerosol concentrations in Eastern China are very high due to both direct emissions and secondary aerosol
9 formation from precursor gases such as NO₂, SO₂ and VOCs. They are produced by anthropogenic activities
10 such as industry, transportation and heating, black carbon and other carbonaceous aerosols produced by
11 biomass burning, dust aerosols produced from the deserts, etc. Aerosol particles influence the local climate
12 such as monsoon intensity and the distribution of precipitation, conversely, monsoon in eastern China also
13 plays an important role in the wet deposition and transport of aerosol particles (Li et al., 2016). The Asian
14 monsoon system plays an important role in the precipitation across the country (Kourtidis et al., 2015). In
15 early April, the pre-monsoonal rain period starts over southern China and the summer monsoon rain belt
16 moves northward to the Yangtze River basin in June. Further, the rain belt arrives in northern China in July
17 and the monsoon rain belt propagates back to southern China in August. The length of the rain season differs
18 between southern and northern China with the migration of the monsoon across China (Song et al., 2011).
19 Based on these characteristics, four regions with different aerosol emission levels and climate
20 characteristics were selected to study the indirect effects of aerosol particles on cloud micro- and
21 macro-physical properties. The Beijing-Tianjin-Hebei (BTH), Yangtze River Delta (YRD) and Pearl River
22 Delta (PRD) urban clusters are characterized as a temperate monsoon climate region, a subtropical monsoon
23 climate region, and a tropical monsoon climate region, respectively. The BTH domain (35.5°N-40.5°N,
24 113.5°E-120.5°E) is an area with high AOD levels due to rapid industrial and economic development (Fig.
25 1). The YRD domain (28°N-33°N, 117°E-122°E) is a major source region of black carbon (Streets et al.,
26 2001; Bond et al., 2004) and sulfate (Lu et al., 2010). The PRD domain (21.5°N-24.5°N, 111.5°E-115.5°E)
27 is an area within the intertropical convergence zone (ITCZ) migration belt, with high anthropogenic aerosol
28 emissions (Streets et al., 2003; Streets et al., 2008; Lei et al., 2011). In addition, one domain (20°N-25°N
29 and 125°E-130°E), which is located in the Eastern China Sea (ECS for short), has been selected as study
30 area for comparison. The ECS domain is relatively clean, but often impacted by aerosol particles transported
31 from the highly industrialized eastern China (Wang et al., 2014). The study period is 4 years, i.e. 2008-2011.



1



2

3

4

5

6

Figure 1. Map of MODIS/AQUA level 3 AOD over Eastern China averaged over the period from 2008 to 2011. The location of the four clusters (three urban and one ocean) studied here (Beijing-Tianjin-Hebei: BTH, Yangtze River Delta: YRD, Pearl River Delta: PRD and Eastern China Sea: ECS) are marked with black rectangles. The inset shows a histogram for the occurrence of AOD values in each of the four clusters during the period 2008-2011.

7

2.2 Data used

8

9 The aerosol and cloud properties used in this study were derived from the MODIS instruments on the
10 Terra and Aqua satellites. Since these instruments are of the same design, errors due to instrument
11 differences are minimal although some differences have been reported due to degradation of
12 MODIS/Terra (Levy et al., 2010; Xiong et al., 2008). The MODIS L3 collection 5.1 data (which was
13 downloaded from <https://ladsweb.modaps.eosdis.nasa.gov/>) provides daily aerosol and cloud parameters
14 on a 1° by 1° spatial grid. The time difference between the Terra and Aqua overpasses is about three
15 hours, with variations due to swath width. In the following, the time difference between the
16 MODIS/Terra and Aqua observations is referred to as the timestep. The application of daily MODIS
17 satellite data on a 1° by 1° spatial grid in this study on aerosol-cloud interaction (ACI) ensures that the
18 aerosol and cloud retrievals are coincident. The MODIS instruments have 36 spectral bands, the first
19 seven of these (0.47- 2.13 μm) are used for the retrieval of aerosol properties (Remer et al., 2005) while
20 cloud properties are retrieved using additional wavelengths in other parts of the spectrum (Platnick et al.,
21 2003). More detailed information on algorithms for the retrieval of aerosol and cloud properties is
22 provided at <http://modis-atmos.gsfc.nasa.gov>. In this study on ACI we use the AOD at 550 nm (referred
23 to as AOD throughout this manuscript), CDR, cloud liquid water path (CWP), cloud optical thickness
24 (COT), cloud fraction (CF), cloud top pressure (CTP) and cloud top temperature (CTT) from both
25 instruments. AOD is used as a proxy for the amount of aerosol particles in the atmospheric column to
26 investigate ACI (Andreae, 2009; Kourtidis et al., 2015). To reduce a possible over-estimation of the
27 AOD, cases with AOD greater than 0.8 were excluded from further analysis. The focus of this study is on
28 warm clouds with CTP greater than 700 hPa, CTT greater than 273K and CWP lower than 200 g m⁻², as
29 most aerosols exist in the lower troposphere (Michibata et al., 2014).

30 In addition, to explore the effect of meteorological conditions on ACI, we use the daily temperature at the
1000 hPa and 700 hPa levels, relative humidity at the 750hPa level and pressure vertical velocity (PVV)



1 at the 750 hPa level. LTS is defined as the difference in potential temperature between the free
2 troposphere (700hpa) and the surface, which is representative of typical thermodynamic conditions
3 (Klein and Hartmann, 1993). These meteorological data were obtained from daily ERA Interim
4 Reanalysis data which contains global meteorological conditions on a grid of $1^{\circ} \times 1^{\circ}$ with 37 levels in the
5 vertical (1000-1 hPa) every six hours (00:00, 06:00, 12:00, 18:00 UTC)
6 (<http://apps.ecmwf.int/datasets/data/interim-full-daily/>). The meteorological properties were resampled
7 to 10:30 (local time) by taking a weighted average of the properties at the two closest times (00:00 UTC
8 and 06:00 UTC) provided by ERA Interim.

9 In this study, high and low AOD are defined as the highest and lowest quartile for each $1^{\circ} \times 1^{\circ}$ location to
10 reduce climatological spatial gradients in aerosol and cloud parameters. As a result, the difference
11 between high and low AOD varies by location. So, for each $1^{\circ} \times 1^{\circ}$ grid cell, 1457 data samples are
12 available for the 4-year study period.

13 3 Method

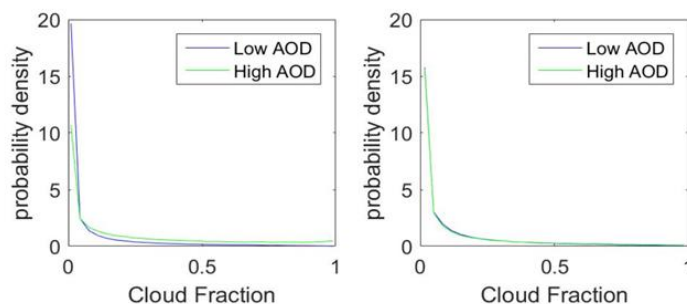
14 3.1 Normalization for initial background

15 For the comparison of the difference in cloud properties in high and in low AOD conditions and the
16 change in this difference during the time step, we need to ensure that the initial conditions are similar, i.e.
17 the probability distributions of a cloud parameter Cloud_X at the start of the time step for the low and
18 high AOD cases should be similar. Any change in this distribution at the end of the time step can then be
19 attributed to changes in cloud properties due to aerosol and/or meteorological effects. To reduce the
20 difference between the initial probability distribution of Cloud_X in high and low AOD conditions at the
21 start of the timestep, normalized histograms of cloud properties and meteorological parameters are made
22 for high and low AOD conditions following the method described by Gryspeerd et al. (2014).

23 It is necessary to reduce possible non-aerosol effects linking cloud properties and AOD at the start time
24 to reveal the strong link between cloud properties and AOD. In Fig. 2 we illustrate the process to remove
25 possible effects linking, as an example, CF and AOD. Normalized histograms of CF are made for the
26 high and low AOD conditions following Gryspeerd et al. (2014) with the difference that in the current
27 study AOD is used instead of AI (Andreae, 2009; Kourtidis, et al., 2015). The CF probability density
28 functions for low and high AOD conditions at the start time are different as illustrated for CF in Fig. 2a.
29 This difference indicates a link between CF and AOD at the start of the time step which needs to be
30 removed to detect the effect of changes during the time step. This is achieved, following the process
31 described in more detail by Gryspeerd et al. (2014). In brief, for each bin data points are drawn out
32 randomly from the conditions with the larger probability density frequency until both distributions match.
33 This is performed independently for each bin and the entire process is repeated until the conditions have
34 sufficiently similar normalised histograms. After that, both conditions have almost the same CF
35 distribution at the start of the timestep through the normalization process, indicating that the non-aerosol
36 effect linking CF and AOD has been removed. This technique has also been applied to ensure that the
37 high and low AOD conditions have the same probability distributions of CDR, COT, CWP and CTP at



1 the start time, even though we find that the normalization for the cloud fraction made the biggest
 2 difference by far. In the further analysis, we only take a subset of original data by removing random
 3 samples until the histograms are similar.



4
 5 Figure 2 Probability density distribution of warm cloud fraction (CF) for low and high AOD conditions. (a) there is a
 6 strong link between AOD and CF before histogram normalization, (b) the link is reduced after histogram
 7 normalization.

8 3.2 The definition of $d(\text{Cloud}_X)$

9 After removal of the potential relationships between AOD and cloud parameters at the time of the Terra
 10 (morning) overpass, as described in Sect. 3.1, effects of aerosol particles on cloud properties are
 11 investigated from the recovery of the relationship between AOD and cloud parameters over the timestep.
 12 For cloud property Cloud_X (CF, COT, CWP, CDR or CTP), the change during the timestep is indicated
 13 by ΔCloud_X . The mean ΔCloud_X for high AOD is then indicated by $\overline{\Delta\text{Cloud}_X[\text{High AOD}]}$ and
 14 similar for low AOD. The difference between the mean change in Cloud_X during the timestep in high
 15 and low AOD conditions is then indicated by $d(\text{Cloud}_X)$:

$$16 \quad d(\text{Cloud}_X) = \overline{\Delta\text{Cloud}_X[\text{High AOD}]} - \overline{\Delta\text{Cloud}_X[\text{Low AOD}]}$$

17 For example, $d(\text{CWP})$ would be the difference between the mean change in CWP in high AOD conditions
 18 minus that in low AOD conditions.

19 The high AOD is representative of polluted atmospheric conditions, and the low AOD is representative of
 20 clean atmospheric conditions. The difference ($d(\text{Cloud}_X)$) between the mean values of the cloud
 21 property Cloud_X during clean (low AOD) and polluted (high AOD) conditions indicates the effect of
 22 these two aerosol cases on the cloud property Cloud_X .

23 4 Results and Discussions

24 4.1 The difference of cloud properties between the low and high AOD at the start time

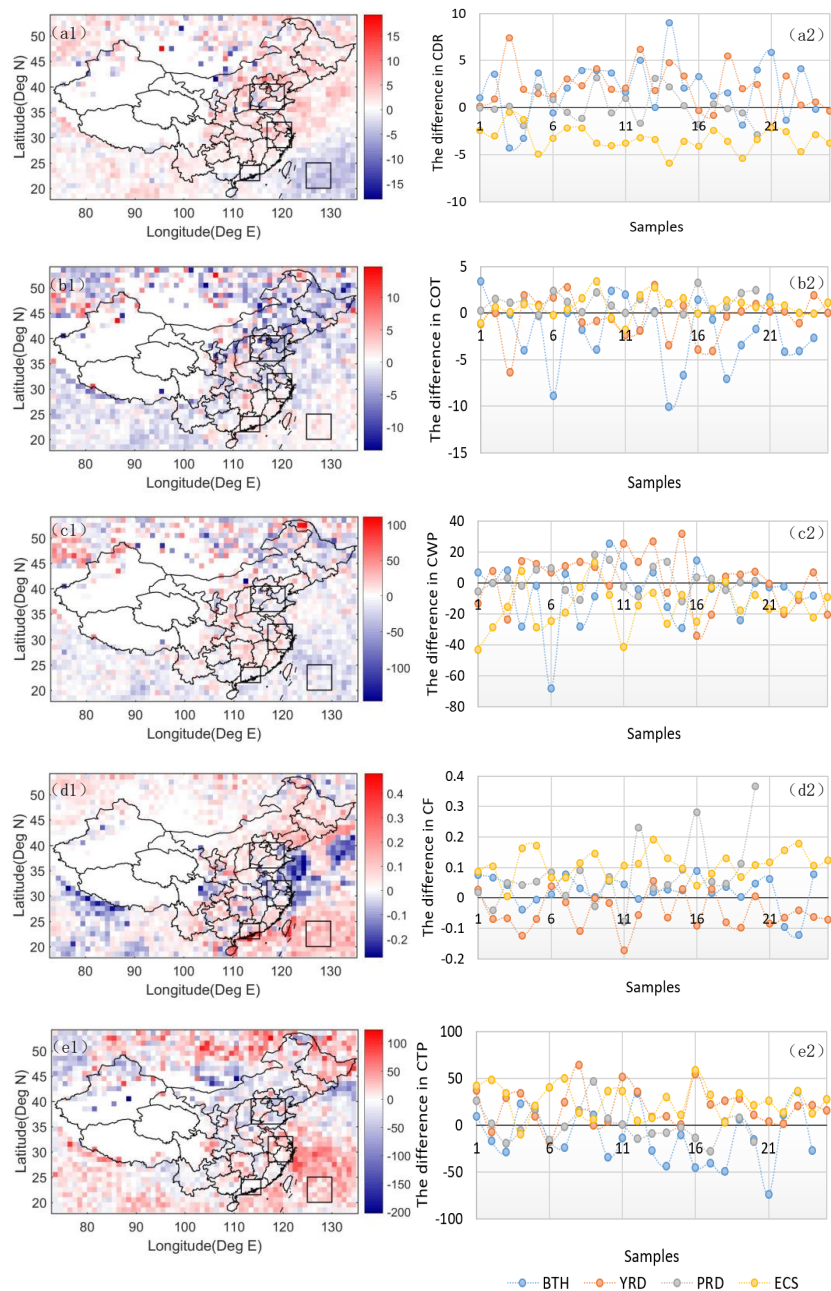
25 The difference in the mean cloud properties (CDR, CF, COT, CWP and CTP) during high and low AOD
 26 conditions at the start time for each $1^\circ \times 1^\circ$ grid cell, i.e.,

27 $\left\{ \overline{\text{Cloud}_X[\text{High AOD}]} - \overline{\text{Cloud}_X[\text{Low AOD}]} \right\}_{t=0}$ represents the change in cloud properties due to the

28 higher AOD. Figure 3 shows the spatial distributions of these differences (left column) and sample series
 29 of the difference for the four regions of interest (right column). The selection of samples for each region is



1 according to the pixels in the region. There are large variations in the response of the cloud parameters to
2 the higher AOD in the four regions. Figures 3(a1-a2) show that over the ECS, CDR is smaller at high
3 AOD than at low AOD, which is consistent with Twomey's effect. In contrast, over the BTH and the YRD
4 urban clusters, CDR is larger at high AOD. This behavior has been observed before for warm clouds in
5 conditions with high AOD (Liu et al., 2017) and may result from the intense competition for the available
6 vapour and the evaporation of smaller droplets as a consequence of the high aerosol abundance over these
7 regions (Wang et al., 2014; Liu et al., 2017). However, over the PRD urban cluster no statistically
8 significant difference in CDR is observed between high and low AOD. For COT (figures 3(b1-b2)) the
9 values are higher at high AOD over the ECS and the PRD, in contrast to the smaller value observed over
10 the BTH and the YRD urban clusters. Likely, this is due to the radiative effect and possible retrieval
11 artefacts as explained in Liu et al. (2017). They inferred that the evaporation of cloud droplets caused by
12 locally absorbing aerosol makes clouds thinner and the presence of absorbing aerosol may reduce the
13 satellite-retrieved COT. Figure 3(c1-c2) shows that CWP is lower at high AOD over the ECS, which is not
14 in agreement with COT variation. In contrast, over the PRD, CWP behaves similar to COT and is higher at
15 high AOD. However, over the BTH and the YRD urban clusters CWP does not show a significant
16 difference between the situations at low and high AOD. Over the ECS, the change in CF between low and
17 high AOD is similar to that of CTP (Figs. 3(d1-d2, e1-e2)): both parameters are larger at high than at low
18 AOD over that area. Meanwhile, over the YRD urban cluster CF is lower and CTP is higher at high AOD.
19 In contrast, over the BTH and the PRD urban clusters CF is higher and CTP is lower at high AOD. Overall,
20 it looks like the aerosol-cloud interactions behave quite similar, over the BTH and YRD urban clusters,
21 both of which have high pollution levels, while over the PRD they show the opposite behavior. The
22 difference in the response of the cloud parameters to low and high aerosol conditions over the four regions
23 may be caused by the difference in pollution levels or pollution types including black carbon, sulphate, sea
24 spray, etc.



1

2 Figure 3 Spatial distribution of the differences in cloud properties (top to bottom: CDR, COT, CWP, CF and CTP)
 3 between the highest and the lowest MODIS AOD quartiles (highest - lowest) at the start time of the timestep
 4 (MODIS/Terra) (left, a1-e1) and sample series of the differences in cloud properties (CDR, COT, CWP, CF and CTP)
 5 between the highest and the lowest MODIS AOD quartiles (highest - lowest) at the start time of the timestep
 6 (MODIS/Terra) (right, a2-e2) over Eastern China for the time period 2008-2011.

7 To better characterize the variation in cloud properties between high and low AOD, Table 1 summarizes the



1 responses of cloud properties to the increasing AOD at the start time for the four study areas. We find that
 2 different regions with various aerosol emission levels and different climate characteristics show different
 3 ACI patterns. Over the ECS region, CDR and CWP in high AOD conditions are smaller than at low AOD, but
 4 COT, CF and CTP are higher. Over the BTH urban cluster, the higher AOD results in higher CDR and CF,
 5 while COT and CTP are smaller. Over the YRD urban cluster, CDR and CTP are larger, but COT and CF are
 6 smaller at high AOD. Over the PRD urban cluster, COT, CWP and CF are larger, but CTP is smaller at high
 7 AOD. Overall, the result implies that the interaction between aerosol particles and clouds is more complex
 8 and less predictable over land (BTH, YRD and PRD) than over ocean (ECS).

9 Table 1 The responses of cloud properties to the increasing AOD

Parameters	AOD	CDR	COT	CWP	CF	CTP
BTH	+	+	-	~	+	-
YRD	+	+	-	~	-	+
PRD	+	~	+	+	+	-
ECS	+	-	+	-	+	+

10 Note: '+' indicates increasing, '-' indicates decreasing and '~' indicates the response of cloud properties to the
 11 increasing AOD is not significant.

12 4.2 The mean change in cloud properties over the timestep for low and high AOD

13 The mean afternoon values of cloud properties in either low or high AOD conditions in each $1^{\circ} \times 1^{\circ}$ grid cell
 14 minus those in the morning for low/high AOD shows the variation of cloud properties during 3 hours of
 15 cloud evolution at low/high aerosol concentrations. Figure 4 presents the spatial distributions (left, a1-e1)
 16 and the sample series (right, a2-e2) of differences in cloud properties (CDR, COT, CWP, CF and CTP) after
 17 this 3-hour period for the lowest MODIS/Terra AOD quartiles. Figure 5 shows the spatial distributions (left,
 18 a1-e1) and sample series (right, a2-e2) of these differences for the highest MODIS/Terra AOD quartiles.

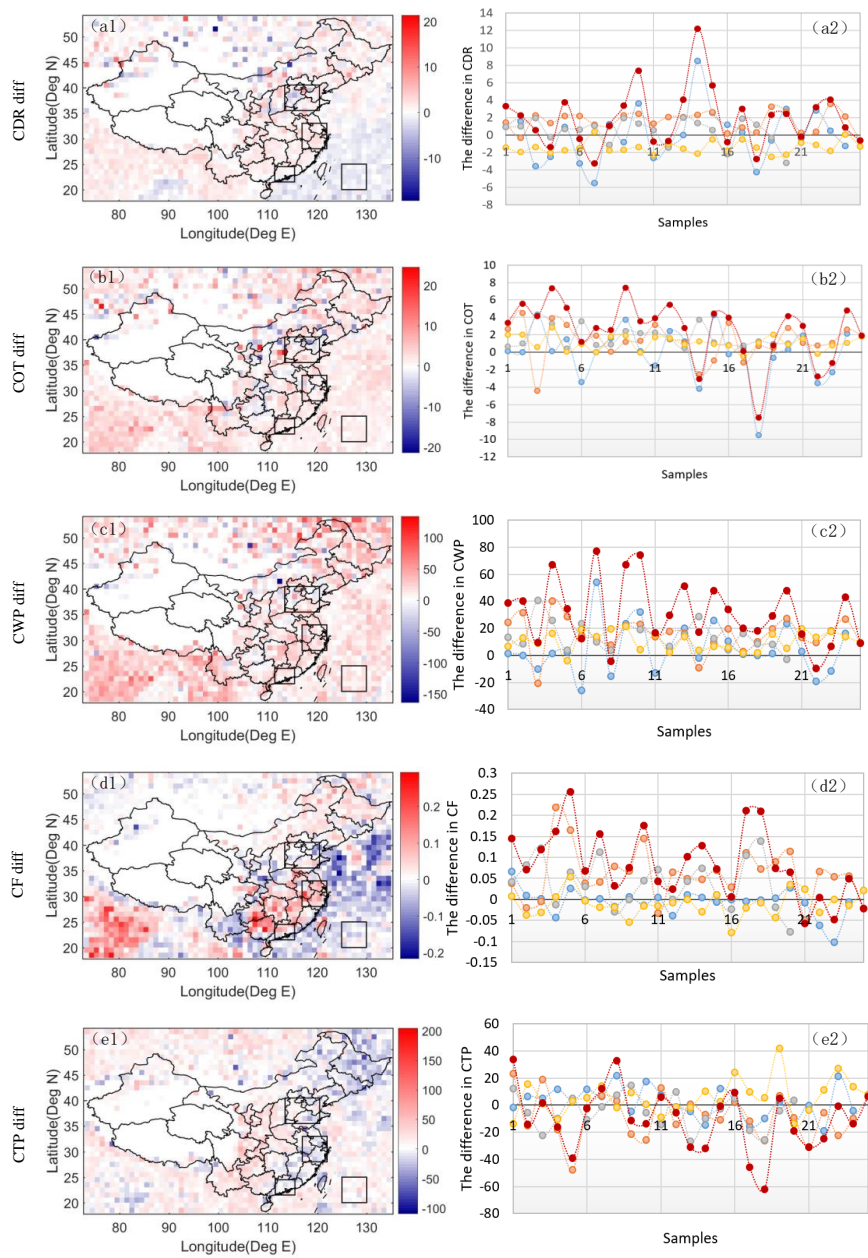
19 Overall, we look at statistics for a large dataset of 4 years. Concerning the effect of aerosol loading on cloud
 20 parameters in each urban cluster, none of the cloud parameters show a significant increase or decrease over
 21 the BTH under either low AOD or high AOD conditions, respectively. For the variations of CDR and CF
 22 over the YRD urban cluster, a significant increase occurs, but for the variation of CTP, a significant
 23 decrease occurs over the YRD for both low and high AOD conditions. By contrast, increases of CDR, COT
 24 and CWP were observed for both low and high AOD conditions over the PRD urban cluster, which is
 25 statistically significant. From the perspective of considering all urban clusters (BTH, YRD and PRD), all
 26 studied cloud properties (CDR, COT, CWP and CF) increase except CTP over land, which decreases during
 27 the timestep, for both low and high AOD (see red samples plot in Figures 4 and 5).

28 Over the ECS, in low AOD conditions, CDR decreases during the timestep while COT and CWP increase
 29 (Figure 4). For high AOD conditions, the variations of the cloud properties (CDR, COT and CWP) during
 30 the timestep are similar to those for low AOD conditions (Figure 5). Furthermore, it appears that COT and
 31 CWP increase more at low AOD than at high AOD. Having a closer look at the CF/CTP variation in both
 32 low and high conditions over ocean, we can find that CF decreases (CTP increases) in low AOD conditions
 33 and CF increases (CTP decreases) in high AOD conditions over ocean, albeit not over ECS.

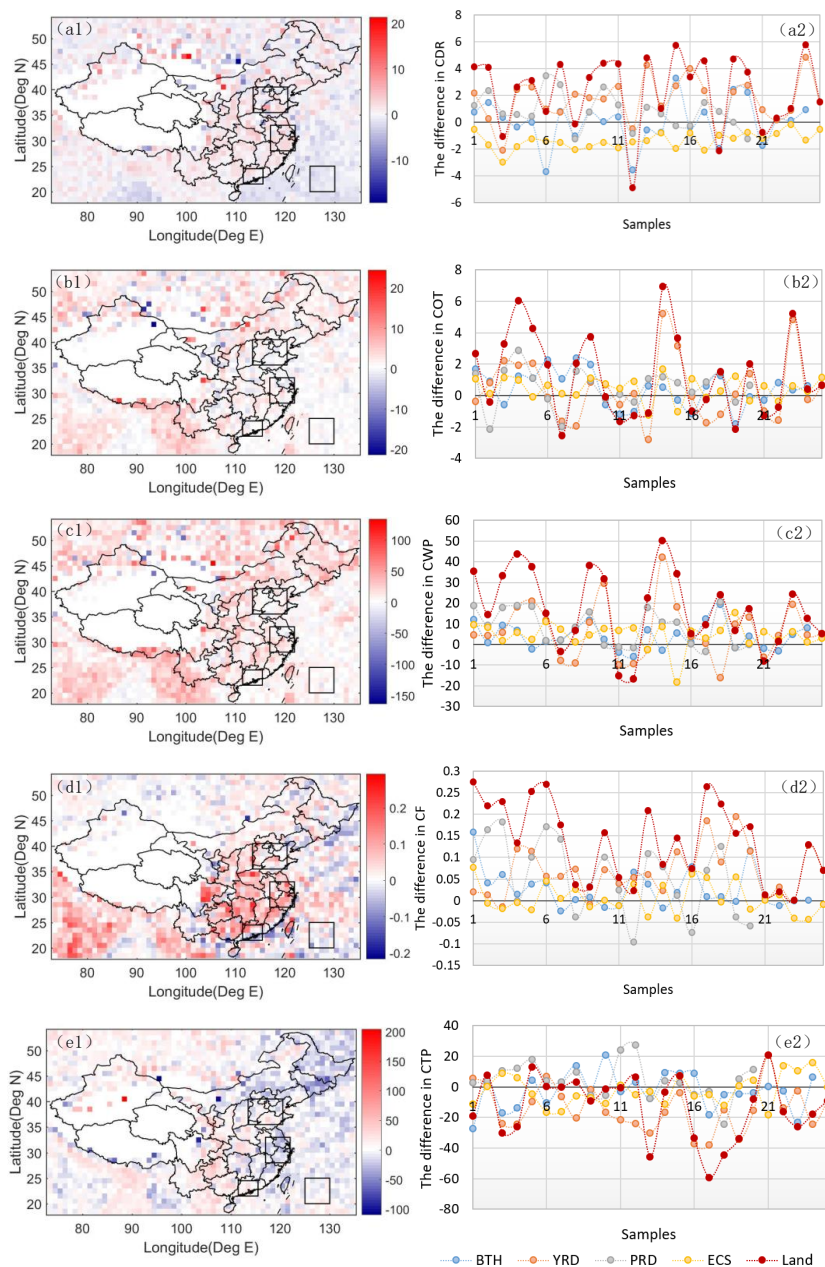
34 In general, the variations in cloud properties over land are similar to those over ocean for both low and high
 35 AOD conditions over 3 hours. Two significant differences are found between land and ocean areas. One is



1 that CDR increases over land but decrease over ocean after the timestep, another significant difference is
2 that CF decreases (CTP increases) for low AOD condition but CF increases (CTP decreases) for high AOD
3 condition over ocean after the timestep, whereas CF increases (CTP decreases) for both low and high AOD
4 conditions over land after the timestep. We can conclude that the variation of cloud properties after 3 hours
5 depends little on the initial AOD over land, even though differences exist among the urban clusters. The
6 increase in afternoon cloud fraction over land is consistent with previous studies concluding that continental
7 warm clouds are likely to be well developed (Wang et al., 2014; Kourtidis et al., 2015). The decrease in
8 afternoon cloud cover over ocean confirms that the largest cover for marine clouds is reached early in the
9 morning (Meskhidze et al., 2009). Table 2 summaries the differences in cloud properties between the Aqua
10 and Terra overpasses for high and low AOD conditions over land and ocean during the time period
11 2008-2011, respectively.



1
2 Figure 4 Spatial distributions of differences in cloud properties (CDR, COT, CWP, CF and CTP) between Aqua and
3 Terra overpasses (3 hours) for the lowest MODIS/Terra AOD quartiles (left, a1-e1). Sample series of the differences in
4 cloud properties (CDR, COT, CWP, CF and CTP) between the values at the start time and the end time of the timestep
5 for the lowest MODIS AOD quartiles (right, a2-e2).



1
2 Figure 5 Spatial distributions of differences in cloud properties (CDR, COT, CWP, CF and CTP) between Aqua and
3 Terra overpasses (3 hours) for the highest MODIS/Terra AOD quartiles (left, a1-e1). Sample series of the differences in
4 cloud properties (CDR, COT, CWP, CF and CTP) between the values at the start time and the end time of the timestep
5 for the highest MODIS AOD quartiles (right, a2-e2).

6
7
8
9



1

2 Table 2 Differences in cloud properties between Aqua and Terra for high and low AOD, over land and ocean.

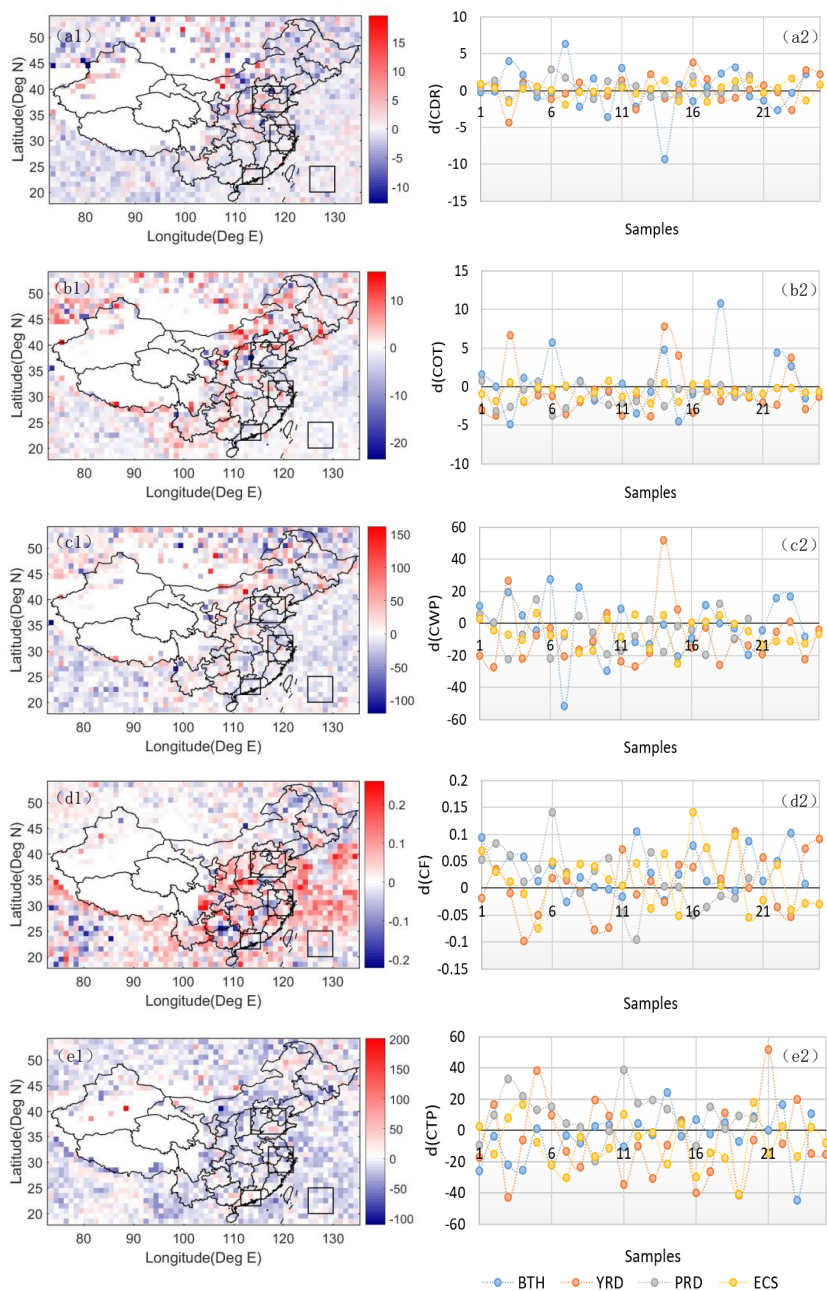
	Land			Ocean		
	L_AOD	H_AOD	d(Cloud_X)	L_AOD	H_AOD	d(Cloud_X)
CDR	+	+	--	-	-	--
COT	+	+	-	+	+	-
CWP	+	+	-	+	+	-
CF	+	+	+	-	+	~
CTP	-	-	-	+	-	-

3 注: '+' indicates increasing, '-' indicates decreasing, '~' indicates the response of cloud properties to the increasing
 4 AOD is not significant or vague. '--' indicates the difference between the mean change in cloud properties (CF, COT,
 5 CWP, CDR and CTP) of the low and high AOD conditions over the timestep is small. L_AOD and H_AOD represent
 6 the low and high aerosol conditions, respectively.

7 4.3 The difference between the mean changes in cloud properties for low and high AOD over the 8 timestep

9 The differences between the mean changes in cloud properties (CF, COT, CWP, CDR and CTP) between
 10 the Terra and Aqua overpasses in high and in low AOD conditions (d(Cloud_X) as defined in section 3.2)
 11 are investigated to identify the effect of aerosol particles on the cloud properties. Figure 6 shows the
 12 differences between the mean change in cloud properties at low and high AOD conditions during the two
 13 observations at 10:30 and 13:30.

14 Figure 6 shows that the values of d(CDR) vary around zero over the three urban clusters, which indicates that
 15 during high and low AOD over land the change in CDR during the three hours between the MODIS/Terra and
 16 Aqua overpasses is similar. Over the ECS the values of d(CDR) also vary around zero, which indicates that
 17 the CDR of high AOD decreases as much as that of low AOD over ocean. Most of the d(COT) values are
 18 negative over the four regions, especially for the PRD and ECS. This shows that the COT increases less in
 19 high AOD conditions than in low AOD conditions, over both land and ocean. Likewise, the values of d(CWP)
 20 are almost all negative over the four regions although over the BTH urban cluster the values are less negative
 21 than over the other clusters and a number of positive values is observed. This indicates that in high AOD
 22 conditions the CWP increases less during the timestep than at low AOD conditions. Meanwhile, the values
 23 of d(CF) are larger than zero over the BTH urban cluster. This shows that the cloud fraction in high AOD
 24 conditions over BTH increases much more than that in low AOD conditions. The value of d(CF) is overall
 25 positive over land, which indicates that over land in high AOD conditions the cloud cover increases much
 26 more than in low AOD conditions. However, compared with the variation of d(CF) over the BTH, the
 27 variations of d(CF) over the YRD, PRD and ECS regions show a less clear pattern with different
 28 behaviors. As regards CTP, we find that the values of d(CTP) are positive over the PRD urban cluster, but
 29 negative over the YRD and ECS regions. In addition, the behavior d(CTP) over the BTH urban cluster is
 30 variable with both negative and positive values. Overall, even though there are large variations of d(CTP)
 31 with increasing AOD over the three urban clusters, it seems that the value of d(CTP) is negative over land,
 32 indicating that in high AOD conditions over land the CTP decreases less than in low AOD conditions. We
 33 can conclude that the variation in d(Cloud_X) is different for continental and oceanic clouds. This applies to
 34 CDR, cloud fraction (CF) and CTP, but not to COT and CWP. Table 2 summarizes the difference between
 35 the mean changes in cloud properties for low and high AOD over the timestep of 3 hours.



1

2

3

Figure 6 Spatial distributions (left, a1-e1) and sample time series (right, a2-e2) of $d(\text{Cloud}_X)$ (as defined in sect. 3.2) for CDR, COT, CWP, CF and CTP over Eastern China during the time period 2008-2011.



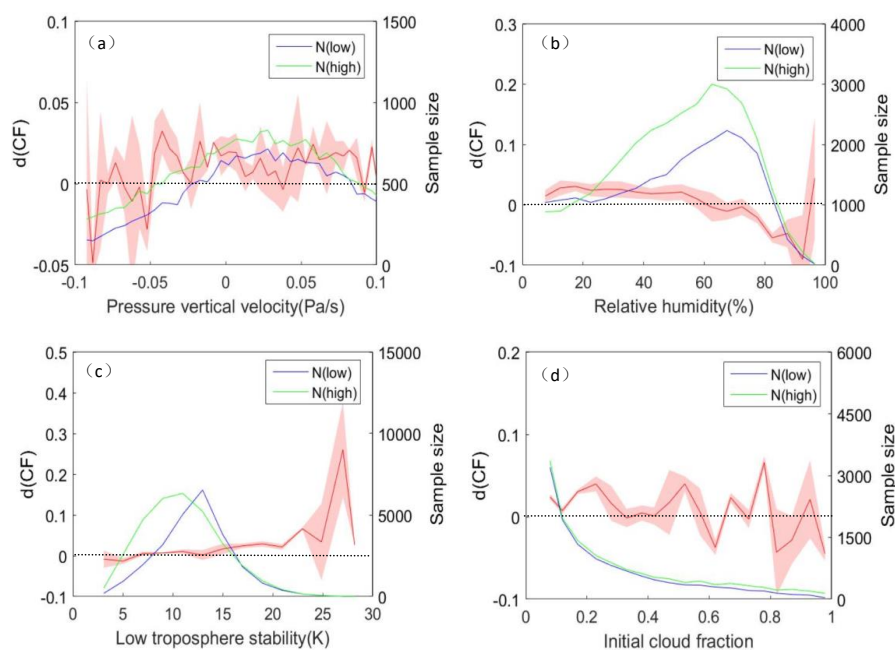
1 4.4 Meteorological effects

2 In order to explore the initial meteorological effects on the correlations between AOD and the cloud
3 fraction, we determine the difference in mean cloud parameters between the high and low AOD
4 conditions at the end of the timestep ($d(\text{Cloud}_X)$) in meteorological variable space rather than in
5 longitude-latitude space. Therefore, we define high and low AOD as the highest and lowest quartile
6 for each bin of meteorological parameters, respectively. Figure 7 shows the effect of meteorological
7 factors (PVV, RH, LST and initial cloud fraction) on the $d(\text{CF})$ over land.

8 The PVV, a measure of dynamic convection strength, is very important for cloud formation. The
9 presence of upward motion, as indicated by negative PVV, can enhance the interaction between aerosol
10 particles and clouds as it makes the ambient environment favorable for cloud formation, and vice versa
11 (Jones et al., 2009). Figure 7(a) shows that the $d(\text{CF})$ increases with the PVV when the PVV is negative.
12 In contrast, the $d(\text{CF})$ decreases with the PVV when the PVV is larger than zero. This indicates that the
13 upward motion of air parcels can enhance the cloud cover much more in conditions with high AOD than
14 in conditions with low AOD. However, the relative increase in cloud cover is smaller in the presence of
15 downward motion of air parcels in high AOD environment than in low AOD environment. Figure 7(b)
16 shows that the $d(\text{CF})$ decreases with increasing RH when RH is lower than 92%. This implies that the
17 cloud cover increases much more in low AOD environment than in high AOD environment with
18 increasing RH. However, when RH is larger than 92%, a strong increase of $d(\text{CF})$ occurs due to
19 activation of CCN and formation of clouds. It should be noted that the variation of $d(\text{CF})$ with increasing
20 RH is uncertain as the sample sizes of high and low AOD conditions are small. The LTS is an indicator
21 for the mixing state of the atmospheric layer adjacent to the surface. It describes to some extent the
22 atmosphere's tendency to promote or suppress vertical motion (Medeiros and Stevens, 2011), which in
23 turn affects cloud properties (Klein and Hartmann, 1993). A positive LTS is associated with a stable
24 atmosphere in which vertical mixing is prohibited; negative PVV indicates local upward motion of air
25 parcels. Figure 7(c) shows that the $d(\text{CF})$ increases with increasing LTS when LTS is lower than 27,
26 but decreases with increasing LTS for higher values. High LTS indicates a strong inversion, which
27 prevents vertical mixing and cloud vertical extent, maintaining a well-mixed and moist boundary layer
28 and providing an environment which favors the development of a low cloud cover, especially in an



1 environment with high AOD concentrations. However, the sample sizes of high and low AOD conditions
2 are small when LTS is higher than 27. Therefore, the relationship between $d(\text{CF})$ and LTS is uncertain.
3 Figure 7(d) shows that there is weak negative relationship between $d(\text{CF})$ and initial cloud fraction. The
4 effect of initial cloud fraction on $d(\text{CF})$ is not clear.



5
6 Figure 7 Variation of $d(\text{CF})$ (red) as function of initial meteorological parameters and cloud fraction for warm clouds
7 over land. The distribution of points for low (blue) and high (green) AOD as a function of meteorological parameters
8 is shown by the solid lines. This plot is composed from MODIS data (including Terra and Aqua) for all warm cloud
9 points over the years 2008-2011. Meteorological parameters are plotted along the horizontal axis, the left vertical
10 axis denotes $d(\text{CF})$ and the right vertical axis denotes the number of high and low AOD samples.

11 5 Conclusions

12 The large anthropogenic emissions in eastern China render this area an important hotspot for studying
13 how cloud microphysical properties are affected by anthropogenic aerosols (Ding et al., 2013). In this
14 work, based on the near-simultaneous aerosol and cloud retrievals provided by MODIS, together with the
15 ERA Interim Reanalysis data, we investigated the effect of aerosol loading, as indicated by AOD, on
16 aerosol-cloud interactions. Aerosol-cloud interaction was studied over three major urban clusters in
17 eastern China and over one area over the Eastern China Sea. These four areas are representative of
18 different climatic regions and pollution levels. Data over these four study areas were collected for the



1 years 2008 to 2011, and analyzed using statistical methods. Both MODIS/Terra and MODIS/Aqua data
2 were used to study the difference of cloud properties between the morning and early afternoon, i.e. with a
3 time difference of 3 hours.

4 In order to reduce the difference of the initial conditions between high and low AOD conditions at the
5 start of the timestep, normalized histograms of cloud properties and meteorological parameters were
6 made for high and low AOD conditions following the method described by Gryspeerd et al., (2014).
7 After that, the difference between cloud properties (CDR, COT, CWP, CF and CTP) in high and low
8 AOD conditions during the Terra overpass at 10:30 LT for each $1^{\circ} \times 1^{\circ}$ grid was investigated. We looked
9 at statistics for the 4-years dataset and found that different regions with various aerosol emission levels,
10 aerosol types and different climate characteristics show different patterns of ACI. The ACI is more
11 complex over land (BTH, YRD and PRD) than over ocean (ECS). Next, the mean change in cloud
12 properties during the 3 hours between the observations in low and high AOD conditions, as provided by
13 the differences in the observations by MODIS/Terra (morning) and MODIS/Aqua (afternoon)
14 overpasses, were examined and differences were analyzed. The results show that in low and high AOD
15 conditions the variation of cloud properties between the two observations behave similarly (increase or
16 decrease). In general, the variation of cloud properties over the urban clusters is similar to that over ocean.
17 Two significant differences are found between land and ocean areas. One is that CDR increases over land
18 but decrease over ocean after the 3-hour period, another significant difference is that CF decreases (CTP
19 increases) for low AOD condition but CF increases (CTP decreases) for high AOD condition over ocean
20 during the timestep, whereas CF increases (CTP decreases) during that period for both low and high
21 AOD conditions over land. Furthermore, we investigated the difference between the mean change in
22 cloud properties (CDR, COT, CWP, CF and CTP) in low and high AOD conditions between the two
23 observations. We found that the variation in $d(\text{Cloud}_X)$ is different for continental and oceanic clouds.
24 This applies to CDR, cloud fraction and CTP, but not to COT and CWP.

25 Constrained by relative humidity and boundary thermodynamic and dynamic conditions, the variation of
26 $d(\text{CF})$ in response to aerosol abundance over land was also analyzed. The results show that the presence
27 of upward motion of air parcels can enhance the cloud cover much more in high than in low AOD
28 conditions. In contrast, the cloud cover increases much more with increasing RH in clean atmospheric
29 conditions than in polluted atmospheric conditions. Meanwhile, stable atmospheric conditions favor the
30 development of a low cloud cover, especially in high AOD conditions. A statistical analysis of the



1 relation between $d(\text{CF})$ and initial cloud fraction shows a weak negative relationship between $d(\text{CF})$ and
2 initial cloud fraction.

3 In summary, whilst we have reduced the error due to meteorological effects on aerosol retrieval,
4 meteorological covariation with the cloud and aerosol properties is harder to remove. As aerosol-cloud
5 interaction is a complex problem, it is important to synergistically use multiple observation products and
6 atmospheric models to explore the mechanisms of aerosol-cloud interaction. Therefore, further analysis
7 can be carried out in future work.

8 **Acknowledgements**

9 This work was supported by the National Key Research and Development Program of China (No.
10 2016YFD0300101), Strategic Priority Research Program of the Chinese Academy of Sciences-A (No.
11 XDA19030402), the Natural Science Foundation of China (No. 31571565,31671585), Key Basic
12 Research Project of Shandong Natural Science Foundation of China (No. ZR2017ZB0422), and the
13 1-3-5 Innovation Project of RADL_CAS (No. Y7SG0700CX). We are grateful to the ease access to
14 MODIS provided by NASA. We also thank ECMWF for providing daily ERA Interim Reanalysis data in
15 our work.

16 **References**

- 17 Albrecht, B. A. (1989).Aerosols, cloud microphysics, and fractional cloudiness, *Science*, 245(4923):
18 1227-1231.
19
20 Andreae, M. O. (2009).Correlation between cloud condensation nuclei concentration and aerosol
21 optical thickness in remote and polluted regions, *Atmospheric Chemistry and Physics*, 9(2): 543-556.
22
23 Bond, T. C., et al. (2004).A technology - based global inventory of black and organic carbon emissions
24 from combustion, *Journal of Geophysical Research: Atmospheres*, 109(D14).
25
26 Ding, A., et al. (2013).Ozone and fine particle in the western Yangtze River Delta: an overview of 1 yr
27 data at the SORPES station, *Atmospheric Chemistry and Physics*, 13(11): 5813-5830.
28
29 Feingold, G., et al. (2001).Analysis of smoke impact on clouds in Brazilian biomass burning regions:
30 An extension of Twomey's approach, *Journal of Geophysical Research: Atmospheres*, 106(D19):
31 22907-22922.
32
33 Grandey, B. and P. Stier (2010).A critical look at spatial scale choices in satellite-based aerosol indirect



- 1 effect studies, *Atmospheric Chemistry and Physics*, 10(23): 11459-11470.
2
3 Gryspeerd, E., et al. (2014). Satellite observations of cloud regime development: the role of aerosol
4 processes, *Atmospheric Chemistry and Physics*, 14(3): 1141-1158.
5
6 Guo, J.-P., et al. (2011). Spatio-temporal variation trends of satellite-based aerosol optical depth in
7 China during 1980–2008, *Atmospheric environment*, 45(37): 6802-6811.
8
9 Hartmann, D. L., et al. (1992). The effect of cloud type on Earth's energy balance: Global analysis,
10 *Journal of Climate*, 5(11): 1281-1304.
11
12 Jones, T. A., et al. (2009). A six year satellite-based assessment of the regional variations in aerosol
13 indirect effects, *Atmospheric Chemistry and Physics*, 9(12): 4091-4114.
14
15 Kaufman, Y. J., et al. (2005). The effect of smoke, dust, and pollution aerosol on shallow cloud
16 development over the Atlantic Ocean, *Proceedings of the National Academy of Sciences of the United*
17 *States of America*, 102(32): 11207-11212.
18
19 Kaufman, Y. J. and I. Koren (2006). Smoke and pollution aerosol effect on cloud cover, *Science*,
20 313(5787): 655-658.
21
22 Klein, S. A. and D. L. Hartmann (1993). The seasonal cycle of low stratiform clouds, *Journal of Climate*,
23 6(8): 1587-1606.
24
25 Koren, I., et al. (2008). Smoke invigoration versus inhibition of clouds over the Amazon, *Science*,
26 321(5891): 946-949.
27
28 Koren, I., et al. (2010). The invigoration of deep convective clouds over the Atlantic: aerosol effect,
29 meteorology or retrieval artifact?, *Atmospheric Chemistry and Physics*, 10(18): 8855-8872.
30
31 Kourtidis, K., et al. (2015). A study of the impact of synoptic weather conditions and water vapor on
32 aerosol–cloud relationships over major urban clusters of China, *Atmospheric Chemistry and Physics*,
33 15(19): 10955-10964.
34
35 Krüger, O. and H. Graßl (2002). The indirect aerosol effect over Europe, *Geophysical Research Letters*,
36 29(19).
37
38 Lei, Y., et al. (2011). Primary anthropogenic aerosol emission trends for China, 1990–2005,
39 *Atmospheric Chemistry and Physics*, 11(3): 931-954.
40
41 Levy, R. C., Remer, L. A., Kleidman, R. G., Mattoo, S., Ichoku, C., Kahn, R., and Eck, T. F.: Global
42 evaluation of the Collection 5 MODIS dark-target aerosol products over land, *Atmos. Chem. Phys.*, 10,
43 10399–10420, doi:10.5194/acp-10-10399-2010, 2010.
44



- 1 Li, Z., et al. (2016), Aerosol and monsoon climate interactions over Asia, *Rev. Geophys.*, 54,
2 doi:10.1002/2015RG000500.
3
- 4 Liu, Y., et al. (2017). Analysis of aerosol effects on warm clouds over the Yangtze River Delta from
5 multi-sensor satellite observations, *Atmospheric Chemistry and Physics*, 17(9): 5623-5641.
6
- 7 Loeb, N. G. and G. L. Schuster (2008). An observational study of the relationship between cloud,
8 aerosol and meteorology in broken low - level cloud conditions, *Journal of Geophysical Research:*
9 *Atmospheres*, 113(D14).
10
- 11 Lu, Z., et al. (2010). Sulfur dioxide emissions in China and sulfur trends in East Asia since 2000,
12 *Atmospheric Chemistry and Physics*, 10(13): 6311-6331.
13
- 14 Matheson, M. A., et al. (2005). Aerosol and cloud property relationships for summertime stratiform
15 clouds in the northeastern Atlantic from Advanced Very High Resolution Radiometer observations,
16 *Journal of Geophysical Research: Atmospheres*, 110(D24).
17
- 18 Matsui, T., et al. (2006). Satellite - based assessment of marine low cloud variability associated with
19 aerosol, atmospheric stability, and the diurnal cycle, *Journal of Geophysical Research: Atmospheres*,
20 111(D17).
21
- 22 Mauger, G. S. and J. R. Norris (2007). Meteorological bias in satellite estimates of aerosol - cloud
23 relationships, *Geophysical Research Letters*, 34(16).
24
- 25 Medeiros, B. and B. Stevens (2011). Revealing differences in GCM representations of low clouds,
26 *Climate dynamics*, 36(1-2): 385-399.
27
- 28 Menon, S., et al. (2008). Analyzing signatures of aerosol - cloud interactions from satellite retrievals
29 and the GISS GCM to constrain the aerosol indirect effect, *Journal of Geophysical Research:*
30 *Atmospheres*, 113(D14).
31
- 32 Meskhidze, N., et al. (2009). Exploring the differences in cloud properties observed by the Terra and
33 Aqua MODIS sensors, *Atmospheric Chemistry & Physics Discussions*, 9(1).
34
- 35 Meskhidze, N. and A. Nenes (2010). Effects of ocean ecosystem on marine aerosol-cloud interaction,
36 *Advances in Meteorology*, 2010.
37
- 38 Michibata, T., et al. (2014). The effects of aerosols on water cloud microphysics and macrophysics
39 based on satellite-retrieved data over East Asia and the North Pacific, *Atmospheric Chemistry and*
40 *Physics*, 14(21): 11935-11948.
41
- 42 Platnick, S., et al. (2003). The MODIS cloud products: algorithms and examples from Terra, *IEEE T.*
43 *Geosci. Remote*, 41, 459-473, doi:10.1109/TGRS.2002.808301.
44



- 1 Remer, L. A., et al. (2005). The MODIS aerosol algorithm, products, and validation, *J. Atmos. Sci.*,
2 62(4), 947 - 973, doi:10.1175/JAS3385.1.
3
- 4 Reutter, P., et al. (2009). Aerosol- and updraft-limited regimes of cloud droplet formation: influence of
5 particle number, size and hygroscopicity on the activation of cloud condensation nuclei (CCN),
6 *Atmospheric Chemistry and Physics*, 9(18): 7067-7080.
7
- 8 Rosenfeld, D. (2000). Suppression of rain and snow by urban and industrial air pollution, *Science*,
9 287(5459): 1793-1796.
10
- 11 Rosenfeld, D., et al. (2014). Global observations of aerosol - cloud - precipitation - climate interactions,
12 *Reviews of Geophysics*, 52(4): 750-808.
13
- 14 Saponaro, G., et al. (2017). Estimates of the aerosol indirect effect over the Baltic Sea region derived
15 from 12 years of MODIS observations, *Atmospheric Chemistry and Physics*, 17(4): 3133-3143.
16
- 17 Song, Y., et al. (2011). Rain-season trends in precipitation and their effect in different climate regions of
18 China during 1961–2008, *Environmental Research Letters*, 6(3): 034025.
19
- 20 Sporre, M., et al. (2014). A long-term satellite study of aerosol effects on convective clouds in Nordic
21 background air, *Atmospheric Chemistry and Physics*, 14(4): 2203-2217.
22
- 23 Stathopoulos, S., et al. (2017). Space-borne observations of aerosol-cloud relations for cloud systems of
24 different heights, *Atmospheric Research*, 183: 191-201.
25
- 26 Stephens, G. L., et al. (2002). The CloudSat mission and the A-Train: A new dimension of space-based
27 observations of clouds and precipitation, *Bulletin of the American Meteorological Society*, 83(12):
28 1771-1790.
29
- 30 Streets, D. G., et al. (2001). Black carbon emissions in China, *Atmospheric environment*, 35(25):
31 4281-4296.
32
- 33 Streets, D. G., et al. (2003). An inventory of gaseous and primary aerosol emissions in Asia in the year
34 2000, *Journal of Geophysical Research: Atmospheres*, 108(D21).
35
- 36 Streets, D. G., et al. (2008). Aerosol trends over China, 1980–2000, *Atmospheric Research*, 88(2):
37 174-182.
38
- 39 Su, W., et al. (2010). An estimate of aerosol indirect effect from satellite measurements with concurrent
40 meteorological analysis, *Journal of Geophysical Research: Atmospheres*, 115(D18).
41
- 42 Twomey, S. (2007). Pollution and the planetary albedo, *Atmospheric environment*, 41: 120-125.
43
- 44 Wang, F., et al. (2014). Satellite observed aerosol-induced variability in warm cloud properties under



- 1 different meteorological conditions over eastern China, Atmospheric environment, 84: 122-132.
- 2
- 3 Webb, M. J., et al. (2006). On the contribution of local feedback mechanisms to the range of climate
- 4 sensitivity in two GCM ensembles, Climate dynamics, 27(1): 17-38.
- 5
- 6 Xiong, X., Wu, A., and Cao, C (2008). On-orbit calibration and inter-comparison of Terra and Aqua
- 7 MODIS surface temperature spectral bands, Int. J. Remote Sens., 29, 5347–5359,
- 8 doi:10.1080/01431160802036300.
- 9
- 10 Yuan, T., et al. (2008). Increase of cloud droplet size with aerosol optical depth: An observation and
- 11 modeling study, Journal of Geophysical Research: Atmospheres, 113(D4).
- 12
- 13